European Journal of Pharmaceutical Sciences 191 (2023) 106597

Contents lists available at ScienceDirect

European Journal of Pharmaceutical Sciences

journal homepage: www.elsevier.com/locate/ejps

How enzymatic hydrolysis of polysorbate 20 influences colloidal protein stability

Nils Glücklich [a,1], Stefan Carle [b,1], Tim Diederichs [b], Julia Buske [b], Karsten Mäder [a], Patrick Garidel [b,c,*]

[a] Institute of Pharmacy, Faculty of Biosciences, Martin-Luther-University Halle-Wittenberg, Wolfgang-Langenbeck-Strasse 4, Halle (Saale) 06120, Germany
[b] Innovation Unit, PDB, Boehringer Ingelheim Pharma GmbH & Co. KG, Birkendorfer Straße 65, Biberach an der Riss 88397, Germany
[c] Institute of Chemistry, Faculty of Physical and Theoretical Chemistry, Martin-Luther-University Halle-Wittenberg, Von-Danckelmann-Platz 4, Halle (Saale) 06120, Germany

ARTICLE INFO

Keywords:
Polysorbate
Tween®
Protein formulation
Free fatty acids
Hydrolysis
HCPs
Lipase
Particle formation
Shaking stability

ABSTRACT

Polysorbates (PS) are esters of ethoxylated sorbitol anhydrides of different composition and are widely used surfactants in biologics. PSs are applied to increase protein stability and concomitant shelf-life via shielding against e.g., interfacial stresses. Due to the presence of specific lipolytic host cell protein (HCP) contaminations in the drug substance, PSs can be degraded via enzymatic hydrolysis. Surfactant hydrolysis leads to the formation of degradants, such as free fatty acids that might form fatty acid particles. In addition, PS degradation may reduce surfactant functionality and thus reduce the protection of the active pharmaceutical ingredient (API). Although enzymatic degradation was observed and reported in the last years, less is known about the relationship between certain polysorbate degradation patterns and the increase of mechanical and interfacial stress towards the API.

In this study, the impact of specifically hydrolyzed polysorbate 20 (PS20) towards the stabilization of two monoclonal antibodies (mAbs) during accelerated shaking stress conditions was investigated. The results show that a specific enzymatic degradation pattern of PS20 can influence the colloidal stability of biopharmaceutical formulations. Furthermore, the kinetics of the appearance of visual phenomena, opalescence, and particle formation depended on the polysorbate degradation fingerprint as induced via the presence of surrogate enzymes. The current case study shows the importance of focusing on specific polysorbate ester fractions to understand the overall colloidal protein stabilizing effect. The performed study gives first insight into the functional properties of PS and helps to evaluate the impact of PS degradation in the formulation development of biopharmaceuticals in general.

1. Introduction

Polysorbates (PS) are widely used as well-tolerated, highly biocompatible, non-ionic surfactants in food and drug preparations (EFSA (European Food Safety Authority), 2015). Within biopharmaceutical formulations, they are used to protect the active pharmaceutical ingredient (API) against e.g., interfacial stresses (Bee et al., 2011; Wang, 1999; Rayaprolu et al., 2018; Garidel et al., 2021). Polysorbates have generally low critical micelle concentration (CMC) ranges from 0.01 to 1 $g{\cdot}l^{-1}$ (Martos et al., 2017; Ehsan et al., 2012; Knoch et al., 2021; Garidel et al., 2021). However, the role of the low surfactant CMC ranges related to protein stabilization is still under debate (Bee et al., 2011; Wang, 1999; Rayaprolu et al., 2018; Garidel et al., 2021). Contrary to most excipients, PSs are not just a defined single chemical entity, but rather a complex mixture of different compounds. A major part of PS compounds is sorbitan and isosorbide cores ethoxylated to POE chains and esterified to fatty acids. In total PS20 is a heterogenous mixture with hundreds of different components. The non-esterified species are not expected to have amphiphilic properties as they are not esterified to hydrophobic fatty acids. The esterified fatty acid composition can vary and is specified for each polysorbate (PS) by the pharmacopeia (USP-NF 2020; Ph.Eur 2020). The main fatty acid esterified in polysorbate 20

* Corresponding author at: Innovation Unit, PDB-TIP, Boehringer Ingelheim Pharma GmbH & Co. KG, Birkendorfer Straße 65, Biberach an der Riss 88397, Germany.
E-mail address: Patrick.Garidel@boehringer-ingelheim.com (P. Garidel).
[1] These authors contributed equally to this work.

https://doi.org/10.1016/j.ejps.2023.106597
Received 13 May 2023; Received in revised form 26 August 2023; Accepted 25 September 2023
Available online 26 September 2023

(PS20) is lauric acid (pH. Eur.: 40–60 %). Other fatty acids with accepted values > 10 % (Ph. Eur.) are mainly myristic acid, palmitic acid, and oleic acid. In addition to the variability of the fatty acid, the degree of esterification can vary, including non-esterified species as well as mono-, di-, tri- and tetra-esters (Evers et al., 2020; Hewitt et al., 2011) (see Fig. 1).

Although PSs reveal several beneficial traits as excipient, two aspects regarding their inherent instability undermine these positive aspects (Wuchner et al., 2023). First, their ester-bond dependent susceptibility regarding hydrolysis during drug storage, which is mainly mediated via residual lipolytic host cell proteins (HCP) in biologics (Roy et al., 2021; Vanderlaan et al., 2018; Honemann et al., 2019; Zhang et al., 2022). Second, their sensitivity towards oxidative stress (degradation pathways are reviewed in detail by Kishore et al. (2011), Dwivedi et al. (2018), Weber et al. (2023), Larson et al. (2020), Donbrow et al. (1978)). The enzymatic-mediated instability leads to the release of free fatty acids (FFA), directly triggering the formation and appearance of fatty acid particles due to their poor solubility in aqueous systems. This is a major quality concern for biopharmaceuticals since they have to be practically free of visible particles according to health authorities (Labrenz, 2014; Glücklich et al., 2020; Doshi et al., 2015). Additionally, the content of esterified PS subspecies with amphiphilic characteristics decreases, which may reduce the protective effect towards the API against interfacial stresses (Grabarek et al., 2020).

There are numerous reports about enzymatic degradation of PSs in liquid formulations of biopharmaceuticals (Chiu et al., 2017; Zhang et al., 2020; Park et al., 2017; Hall et al., 2016). These reports differ in (i) the described degradation kinetic of PSs, (ii) the used proteins and variations in their HCP profile, and (iii) the observation of certain substrate preferences of the involved HCPs towards some PS esters (Chiu et al., 2017; Zhang et al., 2020; Park et al., 2017; Hall et al., 2016). Some HCPs may trigger the degradation of mainly mono-esters (Zhang et al., 2020), whereas others degrade mono- and di-esters (Hall et al., 2016) or only higher-order esters (Roy et al., 2021). Although these differences in degradation patterns are known, only limited, non-connected data are available regarding the consequences for the protein stabilizing properties of the degraded PSs in question.

The objective of this study was to investigate the impact of specific PS20 degradation patterns regarding the stabilization of two model monoclonal antibodies (mAb) in liquid formulations. We assessed whether certain PS20 ester groups, or certain PS20 fractions contribute differently to the overall colloidal protein stabilizing properties. Therefore, three surrogate lipases were used, which degradation fingerprints were investigated in detail in a preceding study, showing a "selected" ester degradation (Glücklich et al., 2021). Lipoprotein lipase (LPL, *Burkholderia* sp.) showed increased hydrolytic activity towards di-esters and multi-esters (Glücklich et al., 2021). Lipase from porcine pancreas type II (PPL F2, *Sus scrofa domesticus*) demonstrated increased hydrolytic activity towards mono-esters, and lipase from porcine pancreas type VI-S (PPL F6, *Sus scrofa domesticus*) showed hydrolytic activity "evenly" distributed between various ester fractions (Glücklich et al., 2021). These three lipases were used to generate formulations with a specifically hydrolyzed PS20 pattern, while keeping the cumulative amount of esterified subspecies constant, thereby changing the subspecies composition. The impact was investigated subsequently in a shaking study to induce interfacial stress on the tested proteins. The samples were analyzed by assessing their visual appearance of particle formation, opalescence, high molecular weight (HMW) species, low molecular weight (LMW) species and monomer content, as well as PS20 content. Comparing the generated data by complementary methods (see below), we obtained information that allowed us to estimate the protein stabilization effect of similar degradation products induced by actual HCPs in antibody formulations.

2. Experimental section

2.1. Materials

The study was performed with polysorbate 20 high purity (HP) grade (PS20, MW = 1′228 g·mol^{-1}), obtained from Croda International Plc. (Snaith, UK). N-phenyl-1-naphthylamine (NPN) reagent grade, L-methionine pharma grade, disodium hydrogen phosphate dihydrate pharma grade, sodium dihydrogen phosphate dihydrate pharma grade, and Brij-35 reagent grade were purchased from Sigma-Aldrich (St. Louis,

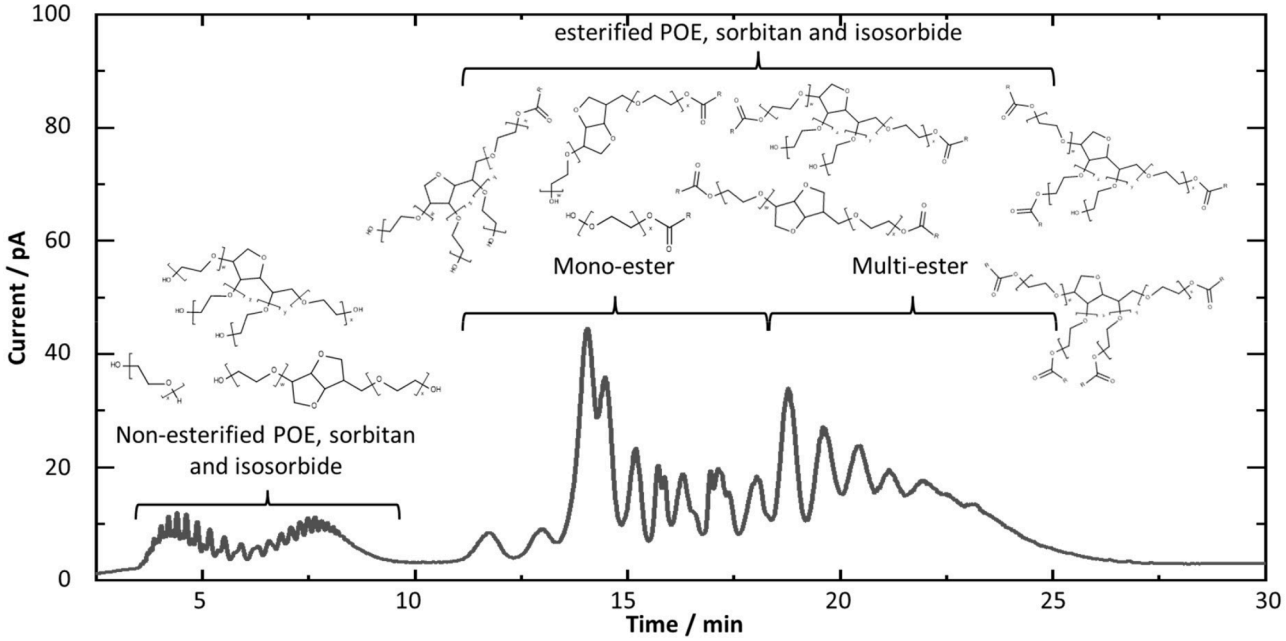

Fig. 1. Polysorbate 20 (PS20) (high purity) fingerprint analyzed via multi-peak charged aerosol detection reversed-phase high performance liquid chromatography (RP-HPLC-CAD). The shown compounds are subspecies of PS20. The fatty acid composition is specific for the different PSs and defined by the pharmacopeias (USP-NF 2020; Ph.Eur 2020). Annotations of the subspecies groups, "non-esterified POE, sorbitan and isosorbide", "mono-ester" and "multi-ester" are based on data from Hewitt et al. (2011) (Hewitt et al., 2011).

MI, USA). Trehalose dihydrate pharma grade was obtained from Pfanstiehl, Inc (Waukegan, USA). Sodium chloride pharma grade was obtained from Dansk Salt A/S (Mariager, Denmark). The buffer agents Tris (hydroxymethyl)aminomethane (TRIS) pharma grade and TRIS HCl pharma grade were purchased from Angus Chemie GmbH (Ibbenbüren, Germany) and 2-(N-morpholino)-ethane-sulfonic acid (MES) reagent grade from Carl Roth GmbH & Co. KG (Karlsruhe, Germany). For pH adjustment, formic acid reagent grade from Thermo Fisher Scientific Inc. (Waltham, MA, USA), acetic acid pharma grade from Merck KGaA (Darmstadt, Germany) or sodium hydroxide reagent grade and hydrochloric acid reagent grade from Grüssing GmbH (Filsum, Germany) were used. Deionized water equivalent to Milli-Q® grade was used to prepare all aqueous solutions. Acetonitrile (ACN) analytical grade was obtained from Carl Roth GmbH & Co. KG (Karlsruhe, Germany). Methanol analytical grade was purchased from Avantor Performance Materials Poland S.A. (Gliwice, Poland).

Both mAbs tested in the shaking studies were provided by Boehringer Ingelheim Pharma GmbH & Co. KG (Biberach an der Riss, Germany). Purified and manufactured mAb1 was supplied in 25 mM acetate buffer at pH 5.5 with a protein concentration of 28 $g{\cdot}l^{-1}$, while mAb2 was supplied in water at 35 $g{\cdot}l^{-1}$.

The used lipases, lipoprotein lipase from *Burkholderia* sp. (LPL), lipase from porcine pancreas type II (PPL F2) and type VI-S (PPL F6), were obtained from Sigma-Aldrich (St. Louis, USA).

The samples were filled in 2 mL type I glass vials provided from Nuova Ompi (Piombino Dese, Italy) and closed with 13 mm fluorotic coated stoppers from Daikyo Seiko (Tochigi, Japan).

2.2. Methods

2.2.1. Hydrolysis of polysorbate with lipases

PS20 was dissolved in water to obtain a pre-stock solution of 200 $g{\cdot}l^{-1}$ PS20. The purchased lipases were dissolved in water (LPL to 0.1 $g{\cdot}l^{-1}$, PPL F2 to 10 $g{\cdot}l^{-1}$ and PPL F6 to 1 $g{\cdot}l^{-1}$). The PS20 pre-stock solution was mixed with lipase and dilution buffer (pH 5.0 or 8.0 depending on the lipase) to obtain a 100 $g{\cdot}l^{-1}$ PS20 stock solution with a defined amount of lipase (LPL to 0.01 $g{\cdot}l^{-1}$, PPL F2 to 1 $g{\cdot}l^{-1}$ and PPL F6 to 0.1 $g{\cdot}l^{-1}$). The used pH is based on the lipase activity preference (PPL F2 shows higher activity at pH 5.0; PPL F6 and LPL show higher activity at pH 8.0) (Glücklich et al., 2021). As lipase free controls, PS20 stock solutions (200 $g{\cdot}l^{-1}$) in respective dilution buffer were prepared and lipase stock solutions were replaced by the same volume of water (final PS concentration: 100 $g{\cdot}l^{-1}$). The mixtures of PS with and without lipases were incubated for 72 h at 25 °C, allowing hydrolysis of the lipase containing PS solution. Subsequently, both types of mixtures (lipase treated and lipase free control) were incubated for 1 h at 80 °C in a water bath to inactivate the lipases. As a second control a non-hydrolyzed and non-heat inactivated PS20 stock solution with 100 $g{\cdot}l^{-1}$ was prepared using water instead of lipase and dilution buffer. The resulting hydrolyzed PS20 (hydrolyzed and heat inactivated lipase containing stocks) as well as the controls (non-heat inactivated and heat inactivated PS20 samples) were analyzed via RP-HPLC-CAD to determine the amount of esterified PS20 species. The PS stock solutions with different lipases result in different hydrolyzation levels as determined with RP-HPLC-CAD. Therefore, the enzymatically hydrolyzed PS20 stock solutions were mixed with intact, heat inactivated PS20 stock solutions of the corresponding pH to obtain a constant hydrolysis level of 20 %. Adjusted PS20 solutions, the heat inactivated placebos (absence of mAb) and the control PS20 were then used for preparation of the final formulations.

2.2.2. Sample preparation for mAb1 and mAb2

The PS20 solutions (Section 2.2.1) and a 5.05-fold spike buffer for trehalose and L-methionine addition were used to obtain various 5-fold spike buffers with 1 $g{\cdot}l^{-1}$ PS20 either partially enzymatically hydrolyzed, heat-stressed, or untreated. For the preparation of the 5-fold spike buffer without PS20 the same amount of water was used instead.

PS-free mAb1 at 25 $g{\cdot}l^{-1}$ in water was supplemented with the 5-fold spike buffers to generate various formulations with a target protein concentration of 20 $g{\cdot}l^{-1}$ and an acetate buffer/trehalose/L-methionine formulation containing 0.2 $g{\cdot}l^{-1}$ (if applicable). For corresponding protein-free solutions (placebos) the protein solution was replaced by the same amount of water. The pH was adjusted with sodium hydroxide or acetic acid to target pH 5.5. For the study in total seven formulations and seven corresponding placebos were used. One without PS20, one with untreated PS20 (not heat inactivated and not hydrolyzed), two with heat inactivated but not hydrolyzed PS20 (stock solutions at varying pH; data not shown) and three differently hydrolyzed and heat inactivated PS20 (lipase containing) solutions adjusted to 20 % hydrolysis of the esterified subspecies. The samples were filled as 1 ml aliquots in 2 ml vials, stoppered and crimped.

Formulations and placebos of mAb2 were prepared in the same way with varying target protein concentration (25 $g{\cdot}l^{-1}$), phosphate buffer/trehalose formulation at pH 6.2 containing PS20 (0.4 $g{\cdot}l^{-1}$) if applicable.

2.2.3. Sample treatment and sampling

The vials were shaken at 25 °C with a Turbula® shaker from Willy A. Bachofen AG Maschinenfabrik (Muttenz, Switzerland) at 67 rpm for up to 120 h. At dedicated sampling time points (6, 24, 48 and 120 h) vials were removed from the shaker and visually inspected. Non-shaken samples (120 h non-shaken) were stored in black boxes protected from light next to the shaker. All incubations were performed at room temperature (RT, ca. 25 °C). After visual inspection (VI) the samples were aliquoted under laminar air flow. Opalescence was measured immediately. Size-exclusion chromatography (SEC), fluorescence micelle assay (FMA), and PS content samples were stored at -70 °C and measured subsequently.

2.2.4. Visual inspection

To monitor the presence of visible particles, caused by e.g., the precipitation of protein, and other phenomena, visual inspection (VI) was conducted. Prior to VI, the sample containers were wiped with a dust-free tissue to remove dust. The analysis was carried out in front of a black and white background on a visual inspection bench according to the Ph. Eur. 2.9.20 (Ph.Eur 2020).

2.2.5. Nephelometric opalescence measurement

The method is based on a nephelometric measurement of scattered light at an angle of 90° ($\lambda = 633$ nm). The measurements were carried out with a custom-made device (Boehringer Ingelheim, Biberach, Germany and Microparts, Dortmund, Germany). For the analysis, a sample volume of 120 µl was inserted into 15 mm single-use glass cuvette. The cuvette was placed in the photometer and the sample measured. Each sample was measured in duplicates ($n = 2$). Values were recorded as formazin nephelometric units (FNU) with a calibration range from 0 to 100 FNU.

2.2.6. Size-exclusion chromatography

Size-exclusion chromatography (SEC) was used to investigate high molecular weight formation induced by the applied shaking stress. Analytics were performed on an UPLC Acquity H-Class— system from Waters (Milford, MA, USA). Samples were diluted with mobile phase (120 mM ammonium sulfate, 200 mM L-arginine, 10 (v/v) isopropanol, pH 7.3) to a protein concentration of 5 $g{\cdot}l^{-1}$. Followed by filtration with 0.2 µm hydrophilic Claristep® Filter from Sartorius Stedim Biotech GmbH (Göttingen, Germany). Per run 6 µl sample with an isocratic gradient and a flow rate of 0.2 $ml{\cdot}min^{-1}$ for 25 min were injected. For separation a Acquity UPLC® BEH200SEC 300 × 4.6 mm, 20 nm column from Waters (Milford, MA, USA) was used. Detection was achieved with an UV detector at 280 nm.

2.2.7. Fluorescence micelle assay

The hydrophobic fluorescence dye NPN incorporates into micelles formed by surfactants. The fluorescence signal increases proportionally with the number of micelles in the solution, allowing to determine the "surfactant" concentration within the sample (Brito and Vaz, 1986). The FMA was adapted from the method described by Lippold et al. (2017) to allow measurement in black, polystyrene, 96-well micro plates (Greiner Bio-One International GmbH, Kremsmünster Austria). Therefore, 240 µl FMA assay buffer containing 5 µM NPN, 0.0015 % (w/v) Brij-35, 150 mM NaCl, 5 % (v/v) ACN and 50 mM Tris–HCl pH 8.0 was added to PS solution with defined concentration (10 µl). The plate was incubated at 35 °C for 1 min at 167 rpm. The samples were measured with a SpectraMax M series fluorescence microplate reader (Molecular Devices, San Josè, USA) for fluorescence with an excitation wavelength of 350 nm and an emission wavelength of 420 nm. The PS concentrations were obtained by using standardized samples for calibration between 0 and 0.6 $g \cdot l^{-1}$ PS.

2.2.8. Reversed phase high-performance liquid chromatography coupled with a charged aerosol detector

Since PSs cannot be detected via traditional absorbance or fluorescence detectors in liquid chromatography, a charged aerosol detector (CAD) was utilized for PS degradation monitoring via liquid chromatography. Therefore, PS content and composition were determined using a Waters Arc™ as reversed phase (RP) high-performance liquid chromatography (HPLC) (Waters Corporation, Milford, MA, USA) coupled with a Corona™ Veo™ RS CAD from Thermo Fisher Scientific Inc. (Waltham, MA, USA). The method was adapted from Hewitt et al. (2011). Briefly, a mixed mode column (Waters Oasis Max 30 µm, 2.1 × 20 mm column) was used for solid phase extraction (SPE) and protein removal followed by a RP analytical column (Zorbax 300 SB – C8 4.6 × 50 mm, 5 µm) for separation of PS subspecies according to their hydrophobicity. The column oven was kept at 50 °C. CAD evaporation temperature was 40 °C. A flow rate of 0.5 $ml \cdot min^{-1}$ was kept during the whole run. Per run 40 µl sample were injected into the system. The sample was washed with 100 % mobile phase A (water with 2 % formic acid). After 5 min the valves switched from waste to the RP column. Elution started with 80 % mobile phase A and 20 % mobile phase B (ACN) for 3.4 min. From 8.4 min to 28 min a linear gradient to 100 % mobile phase B was used, followed by 5 min 100 % mobile phase B. The column was then primed with 100 % mobile phase A until 40 min run time. The chromatograms were baseline corrected using water injections. PS subspecies peak assignment was performed according to the LC-MS data from Hewitt et al. (2011).

3. Results and discussion

3.1. Hydrolysis of polysorbate

Recently, we investigated the substrate preferences, regarding the varying ester subspecies of PS20, as well as preferred reaction conditions of the used lipases (Glücklich et al., 2021). The lipase-treated PS20 stock solutions were analyzed via —RP-HPLC-CAD and subsequently adjusted with non-treated PS20 stock solution to obtain comparable levels of esterified subspecies in each formulation, which led to approx. 20 % enzymatically degraded esters compared to the non-treated stock solution (Fig. 2). In non-treated PS20 samples, peak areas of mono-esters and multi-esters are approximately the same (ratio of approx. 50 % per ester group). Upon treatment with lipases, the overall content of esterified subspecies decreases, while non-esterified subspecies increase (Fig. 2). Thereby, the degradation pattern is highly lipase specific, which also influences the ratio of mono- to multi-esters. For example, results from this study show that PS20 treated with LPL has a ratio of 80 % mono-esters and 20 % multi-esters, due to the preference of LPL for multi-esters. It is worth mentioning that the hydrolysis of higher-order esters leads to the formation of lower-order esters. Depending on the lipase kinetics and substrate preferences, this can lead to the accumulation of mostly mono-esters during degradation, as shown for PS20 degraded with LPL, which has more sorbitan monolaurate than the original PS20 stock solution (Fig. 2, shown in blue). Contrary to LPL, PPL

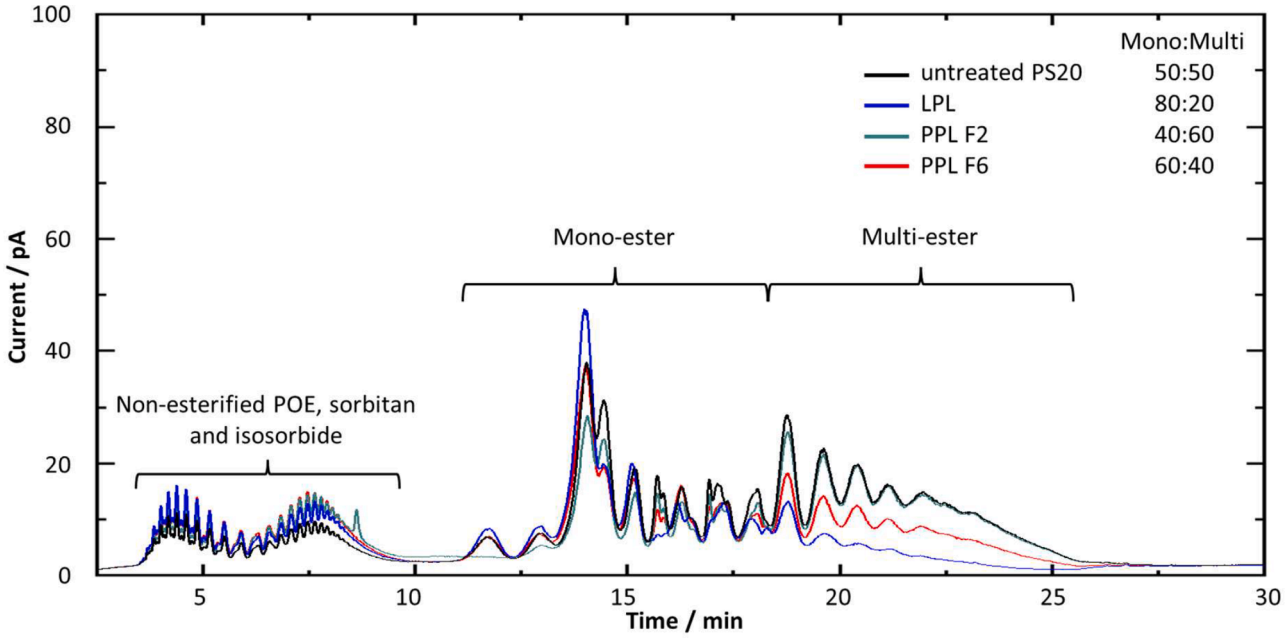

Fig. 2. Chromatographic overlays of non-hydrolyzed and hydrolyzed polysorbate 20 high purity (HP) grade (PS20) samples adjusted to an enzymatic hydrolysis level of 20 %. Chromatograms were generated via multi-peak charged aerosol detection reversed phase high-performance liquid chromatography (—RP-HPLC-CAD). Samples were either incubated without lipase (shown in black) or with lipoprotein lipase (LPL, shown in blue), porcine pancreas lipase type II (PPL F2, shown in green) or porcine pancreas lipase type VI (PPL F6, shown in red). The ratio of mono-esters (peak integration between 11 and 18.5 min; Mono) to multi-esters (peak integration between 18.5 and 27 min; Multi) is given as% of the area within the cumulative area of esterified PS20 subspecies in the elution time range between 11 and 27 min). POE = Polyoxyethylene.

F2 showed strong hydrolysis preference for mono-esters, which shifted the ratio to 40 % mono-esters and 60 % multi-esters. PPL F6 on the other hand, led to the degradation of mono-esters and multi-esters without an exceed of certain mono-esters. This led to a ratio of 60 % mono-esters and 40 % multi-esters in the final PPL F6 treated PS20 stock solutions used for formulation.

3.2. Visual appearance, particle formation and opalescence

Visual appearance was assessed directly by comparing the sample vials for all sampling time points with a vial filled with pure water during the shaking study to evaluate the impact of the applied stress (Fig. 3). Afterwards, the samples were aliquoted and directly used for opalescence measurements (Fig. 4).

Generally, all samples of mAb1 showed a slight, visible opalescence at every sampling time point independent of the presence of PS20 compared to the water vial (Fig. 3A). The control without PS20 (w/o PS20) showed protein precipitation after 6 h of shaking (data not shown) with a drastic increase of white particles after 48 h (Fig. 3A), while the non-shaken sample remained unchanged (no particle formation) over the experimental time of 120 h. No apparent visible changes were observed for any of the mAb1 samples spiked with 0.2 $g \cdot l^{-1}$ PS20 after 120 h of shaking (Fig. 3A), showing that the presence of PS20 stabilizes the mAb1 for the tested formulation. Also, the lipase treated PS samples show no differences to the non-hydrolyzed PS20 control (Fig. 3A). However, opalescence measurements revealed differences between the PS20 containing mAb1 formulations (Fig. 4A). While the non-hydrolyzed control showed relatively constant levels of 12 FNU for all sampling time points up to 120 h, LPL treated samples had an initially higher opalescence, which remained constant for non-shaken samples. Initially, shaking reduced the opalescence in LPL treated samples as observed for the 6 h sampling time point from 15 to 13 FNU, followed by an increase in opalescence up to 17 FNU at the 120 h time point. Such phenomenon, of reduced opalescence are observed when initially the formation of larger visible particles is favored. Depending on the physical properties of the larger particles, further shaking may homogenize the particles leading to an increase of opalescence. mAb1 formulations containing PPL F2 treated PS20 showed only a small increase over the shaking period from 12 to 13 FNU, while PPL F6 treated PS formulations started approx. at the same level as the non-hydrolyzed control (12 FNU), followed by a steady increase in opalescence during shaking up to 17 FNU (compare Fig. 4A). In accordance with the visual inspection, the mAb containing, however, PS20 free control sample (w/o PS20) exceeded the calibration range of the turbidimeter after 6 h of shaking indicating a strong formation of protein particles (Fig. 4A).

Similar to mAb1, the mAb2 formulations showed a slightly opalescent appearance in the visual inspection (Fig. 3B). Furthermore, shaking led to evident, visible changes, both in the control without PS20 as well as in samples spiked with the surfactant. After 48 h of shaking, all samples spiked with lipase treated PS20 started to become opalescent, while the non-hydrolyzed PS20 sample stayed clear. After 120 h of shaking, even the mAb2 formulations with the non-treated PS20 showed evident opalescence, indicating overall higher sensitivity of mAb2 towards shaking compared to mAb1.

These visual trends could be confirmed with the opalescence measurements (Fig. 4B). The mAb2 formulation with non-hydrolyzed PS20 showed constant opalescence of approx. 14 FNU for 48 h. After 120 h sample shaking, the opalescence exceeded the calibration range of the assay for all mAb2 formulations having opalescence values above 100 FNU (Fig. 4B), in agreement with the VI results. The time-dependent increases, however, showed relevant differences between the different lipase treated PS samples and the non-hydrolyzed PS samples. The LPL treated mAb2 formulation had elevated starting levels of approx. 24 FNU, followed by a small drop of opalescence after 6 h with a subsequent rise to 27 FNU after 24 h and 45 FNU after 48 h of shaking. PPL F6 mAb2 formulations started at non-hydrolyzed PS20 control levels (approx. 14 FNU) and followed nearly the same trend as the LPL treated formulations with a faster increase, leading to 20, 35 and 54 FNU at 6, 24 and 48 h of shaking, respectively. First apparent changes in opalescence for PPL F2 treated mAb2 formulations were detected after 48 h of shaking.

Generally, placebos corresponding to the mAb1 and mAb2 formulations appeared visually clear and no changes at all sampling time points for shaken and non-shaken samples were observed (data not shown). Overall, opalescence levels were in the range of 0 to 3 FNU except for placebos spiked with LPL treated PS20 (Fig. 4C and D). Here, both placebos showed initially higher opalescence levels of 5 FNU for the mAb1 placebo and about 10 FNU for the mAb2 placebo, which stayed relatively constant when not shaken (120 h). Shaking on the other hand decreased the opalescence over the course of the study. One explanation for the increased opalescence in LPL treated placebo samples could be the preferential degradation of multi-esters, which leads to a correspondingly higher amount of FFA in the solution. FFA can generate particles in aqueous solutions above their solubility limit, increasing the opalescence (Glücklich et al., 2020; Doshi et al., 2015). The solubility limit is highly dependent on various factors, like surfactant concentration, temperature, and pH. The solubility of fatty acids depends strongly on their deprotonation and therefore on the pH and pKa values. Interestingly, the apparent values of long chain fatty acids depend on the local environment and can vary between 4 and 11 (Heider et al., 2016). Shaking could shift the equilibrium and therefore dissolve some of the generated fatty acid particles, reducing the opalescence in the shaken placebos. Furthermore, one can also consider that

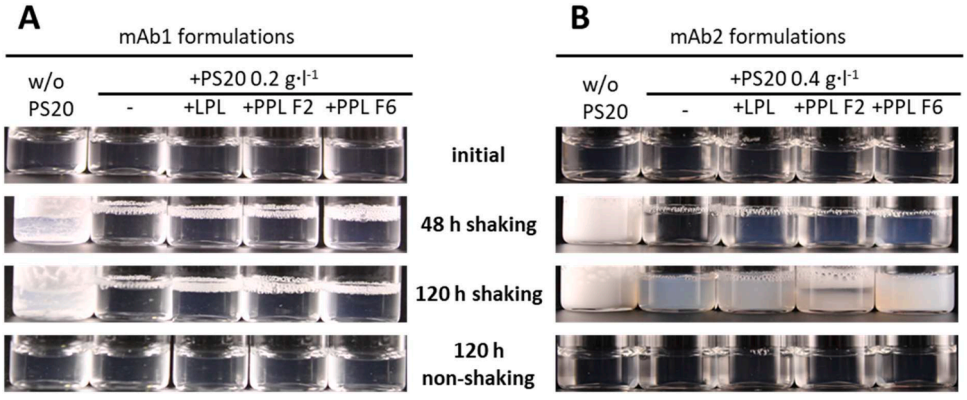

Fig. 3. Visual appearance of formulations of mAb1 (A) and mAb2 (B) shown at the initial sampling time point, after 48 and 120 h of shaking, as well as 120 h without agitation. Formulations were either not spiked with polysorbate 20 HP (PS20; w/o PS20), with PS20 non-hydrolyzed (-) or with enzymatically hydrolyzed PS20 (lipoprotein lipase (LPL), porcine pancreas lipase type II (PPL F2), porcine pancreas lipase type VI (PPL F6)). mAb1 formulations contained 20 $g \cdot l^{-1}$ protein and 0.2 $g \cdot l^{-1}$ PS20. While mAb2 formulations contained 25 $g \cdot l^{-1}$ protein and 0.4 $g \cdot l^{-1}$ PS20.

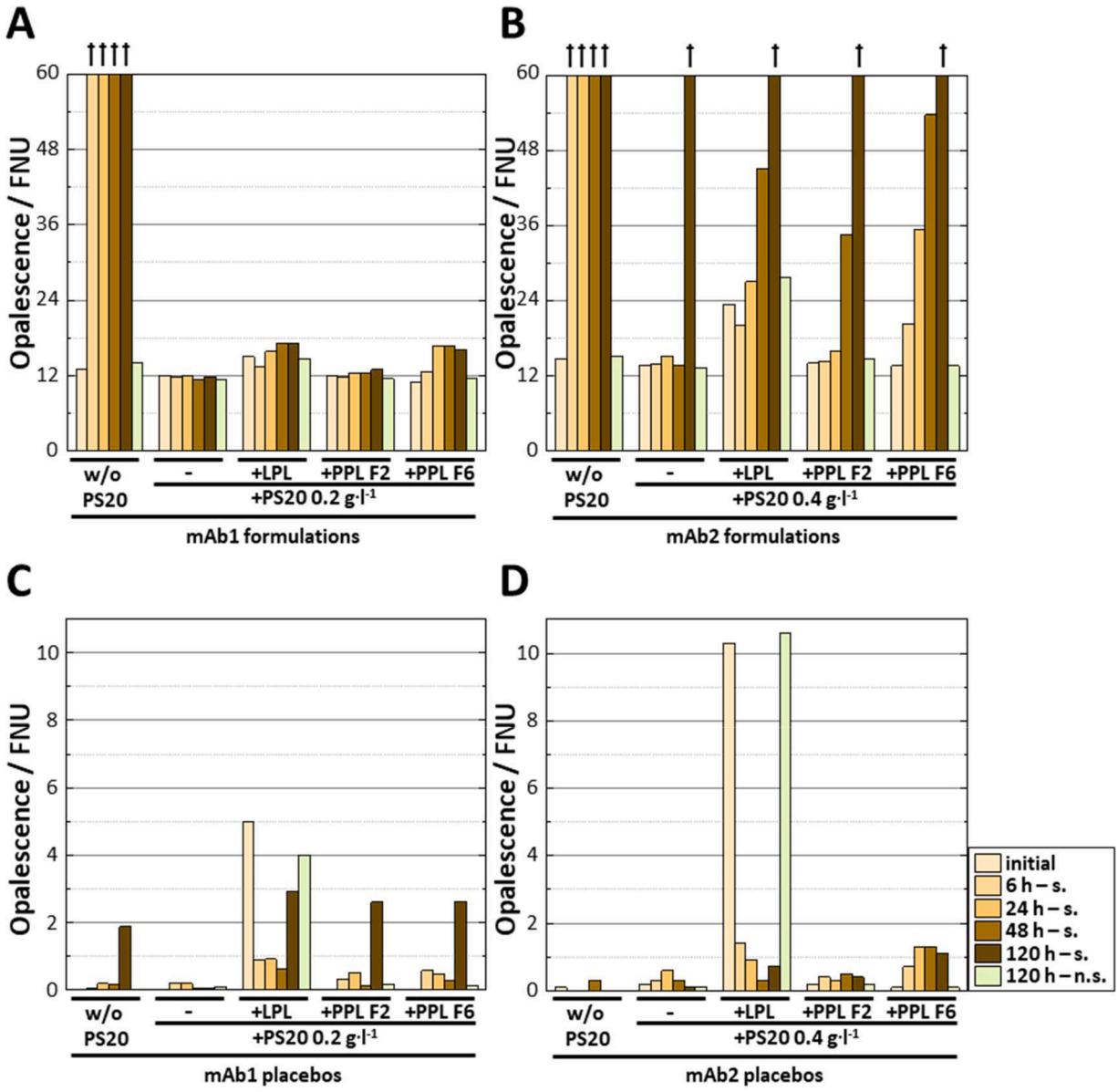

Fig. 4. Opalescence determination via nephelometric measurement. Formazin nephelometric units (FNU) are plotted for the tested formulations and placebos of mAb 1 (A and C, respectively) and mAb 2 (B and D, respectively). Formulations were either not spiked with polysorbate 20 (PS20; w/o PS20), with PS20 non-hydrolyzed (-) or with enzymatically hydrolyzed PS20 (lipoprotein lipase (LPL), porcine pancreas lipase type II (PPL F2), porcine pancreas lipase type VI (PPL F6)). mAb1 formulations contained 20 $g \cdot l^{-1}$ protein and 0.2 $g \cdot l^{-1}$ PS20. While mAb2 formulations contained 25 $g \cdot l^{-1}$ protein and 0.4 $g \cdot l^{-1}$ PS20. Corresponding placebos did not contain any mAb, but the same amounts of PS. The different sampling time points and conditions (shaken = s.; non-shaken = n.s.) are shown in the legend at the bottom right. Samples exceeding the calibration range of the method are depicted with an arrow on top of the bar. Be aware of the different y-axes scales.

the FFA are incorporated into PS20 micelle structures, leading to the formation of mixed micelles, that could prevent the precipitation of FFA (Glücklich et al., 2020; Doshi et al., 2015).

3.3. Monomer and high molecular weight species content via size-exclusion chromatography

UPLC-SEC was used to monitor the formation of high molecular weight (HMW) species of the tested mAbs, which is often a consequence of colloidal instability after shaking of biologics (Kiese et al., 2008; Sluzky et al., 1992). Therefore, monomer as non-aggregated and intact mAbs as well as HMWs as evidence for protein particle formation were investigated (Fig. 5).

Generally, the monomer content (Fig. 5A) of non-stressed mAb1 was very high (100 % at the initial time point for all formulations) and did not change over the study time for non-shaking conditions (120 h) for all tested formulations. Furthermore, stress induced changes were proportional to the rise of HMWs (Fig. 5C). Shaking induced HMW formation varied strongly depending on the formulation. In the control sample without PS20 a steady increase of HMWs up to 80 % after 120 h of shaking was observed (Fig. 5C). Upon the presence of 0.2 $g \cdot l^{-1}$ PS20 the HMW formation was negligible. In samples with non-hydrolyzed PS20 the HMW and monomer content changed marginally, leading to the presence of approx. 2 % HMW. For mAb1 formulations spiked with lipase treated PS20 the HMW content increased to 4, 7 and 10 % for PPL F2, LPL and PPL F6, respectively over a shaking period of 120 h at RT. mAb2 showed overall lower levels of monomer already at the initial time point ranging from 84 % for the formulation without PS20 to

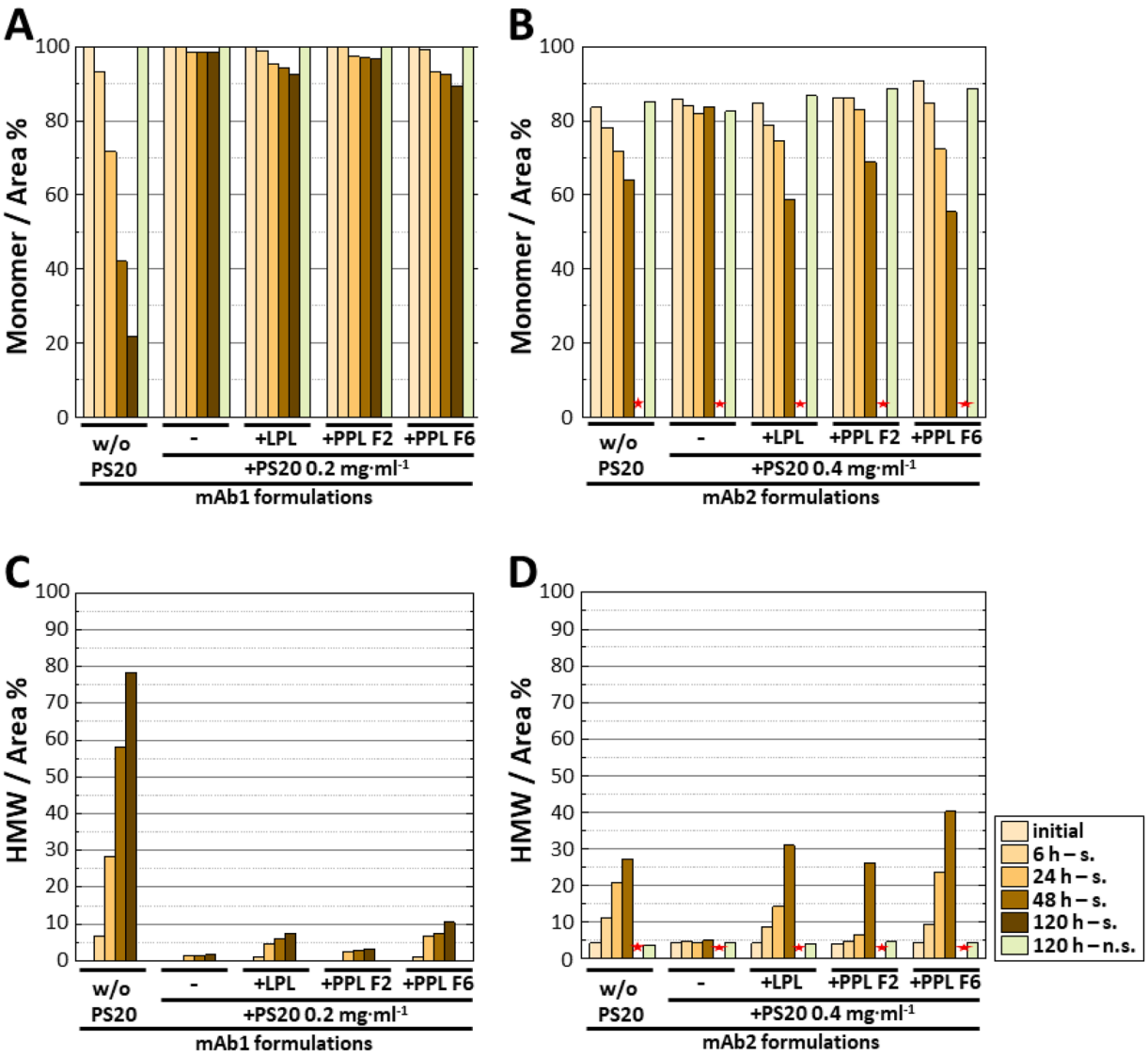

Fig. 5. Monomer and high molecular weight species (HMW) content by size-exclusion chromatography (SEC). The areas compared to the total areas [area%] are plotted for the tested formulations of mAb 1 (A and C) and mAb 2 (B and D). Formulations were either not spiked with polysorbate 20 (PS20; w/o PS20), with PS20 non-hydrolyzed (-) or with enzymatically hydrolyzed PS20 (lipoprotein lipase (LPL), porcine pancreas lipase type II (PPL F2), porcine pancreas lipase type VI (PPL F6)). mAb1 formulations contained 20 $g \cdot l^{-1}$ protein and 0.2 $g \cdot l^{-1}$ PS20. While mAb2 formulations contained 25 $g \cdot l^{-1}$ protein and 0.4 $g \cdot l^{-1}$ PS20. The different sampling time points and conditions (shaken = s.; non-shaken = n.s.) are shown in the legend at the bottom right. Samples marked with a red asterisk are excluded because the sample could not be analyzed due to strong precipitation of the protein.

approx. 90 % for formulations spiked with PPL F6 treated PS20 (Fig. 5B), demonstrating a higher variability and instability of mAb2. Furthermore, mAb2 showed strong, visible protein precipitation after 120 h of shaking independent of the formulation, which made SEC analytics at this time point not feasible (Fig. 5B, asterisk). Initial levels of mAb2 HMW were at approx. 4 % and stayed constant for non-shaken samples. The monomer levels were not entirely proportional to the HMW content (Fig. 5D) due to noticeable amounts of LMWs (data not shown), which were basically absent in mAb1. During the shaking study, however, the LMW amount for mAb 2 did not change (data not shown).

Similar to mAb1, mAb2 showed a gradual increase of HMWs during shaking without the addition of PS20, leading to HMW contents of 11, 21 and 27 % for the 6, 24 and 48 h time points, respectively. However, in contrast to mAb1, non-hydrolyzed PS20 only protected mAb2 from aggregation for the first 48 h of shaking. After 120 h of shaking stress, protein precipitation was here also visible and SEC analysis could not be performed due to the high precipitation as mentioned before. Regarding formulations spiked with lipase stressed PS20, the aggregation patterns were similar for mAb2 as for mAb1. The fastest HMW increase was observed for mAb2 formulations spiked with PPL F6 treated PS20, leading to rising HMW content of 9, 24 and 40 % within 48 h of shaking. This was followed by formulations previously treated with LPL and respective values of 9, 14 and 31 %. The slowest increase of HMW in the first 48 h of shaking for the lipase spiked samples was seen in mAb2 formulation samples with PPL F2 treated PS20 (HMW content of 5, 7 and 26 %). Comparable to mAb1, non-shaken mAb2 controls stayed constant during the 120 h incubation time.

3.4. Polysorbate 20 content and characterization

To monitor the PS20 content, we used two different methods. First, FMA (Fig. 6) was used, which allows a high analytical throughput for the surfactant quantification using microplates, and the second assay relies on more analytically complex —RP-HPLC-CAD (Fig. 7) to get specific structural information on the polysorbate composition. —RP-HPLC-CAD is able to differentiate between non-esterified and esterified PS20

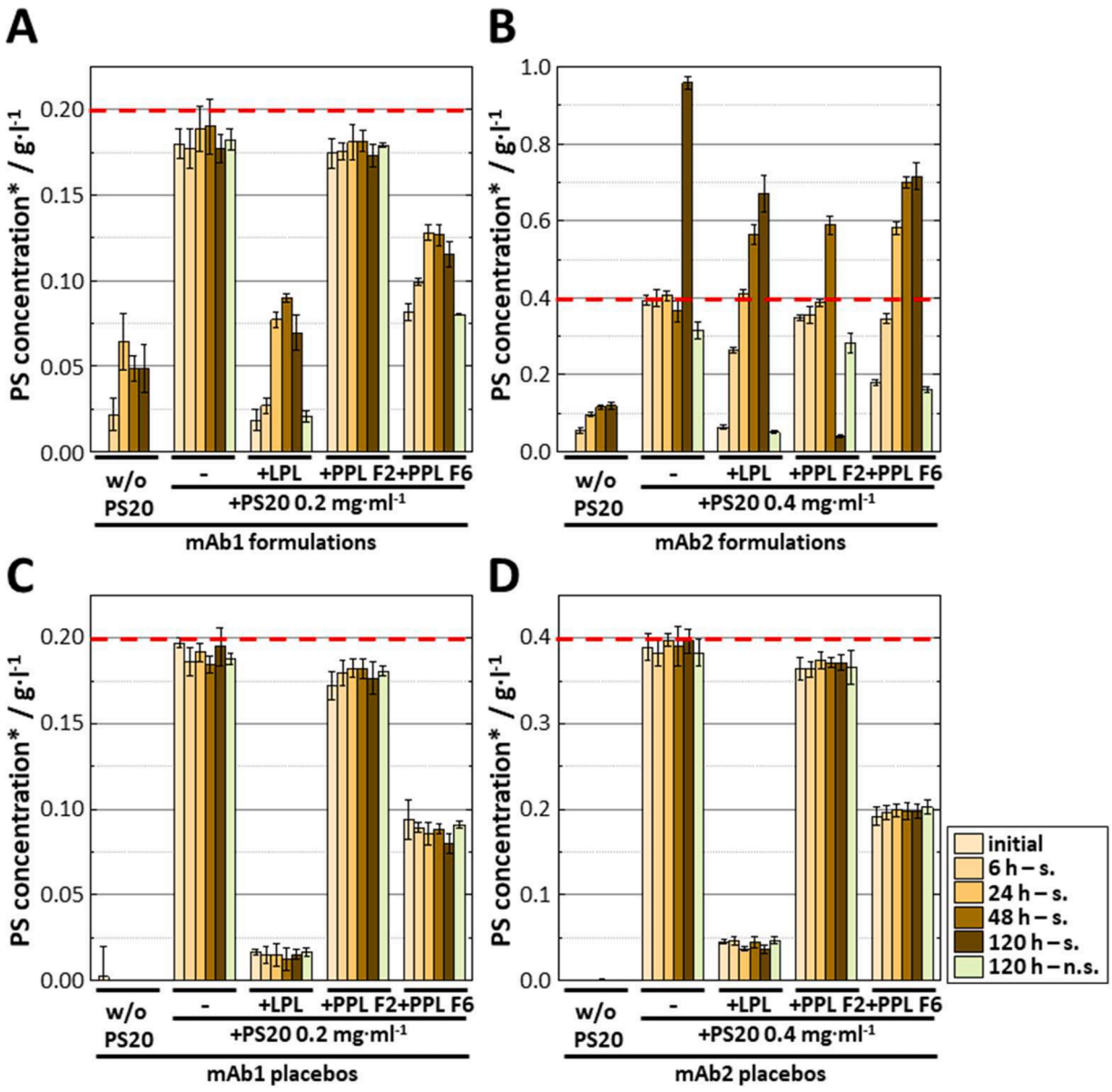

Fig. 6. Polysorbate 20 (PS20) content determined via fluorescence micelle assay (FMA). Apparent PS concentrations in g•l^{-1} are depicted versus tested formulations and placebos of mAb 1 (A and C, respectively) and mAb 2 (B and D, respectively). Formulations were either not spiked with polysorbate 20 (PS20; w/o PS20), with PS20 non-hydrolyzed (-) or with enzymatically hydrolyzed PS20 (lipoprotein lipase (LPL), porcine pancreas lipase type II (PPL F2), porcine pancreas lipase type VI (PPL F6)). mAb1 formulations contained 20 g·l^{-1} protein and 0.2 g·l^{-1} PS20. While mAb2 formulations contained 25 g·l^{-1} protein and 0.4 g·l^{-1} PS20. Corresponding placebos did not contain any mAb, but the same amounts of PS. The target PS20 concentrations (g·l^{-1}) are annotated as red dotted horizontal line. The different sampling time points and conditions (shaken = s.; non-shaken = n.s.) are shown in the legend at the bottom right. The PS20 concentrations are determined as apparent (via asterisk) due to the possibility of false positive signals induced by protein aggregates and particle formation.

subspecies and allows therefore further characterization of the polysorbate fractions (see Fig. 1).

FMA uses a hydrophobic dye, which incorporates in the hydrophobic core of the micelles leading to a rise in fluorescence signal that is proportional to the amount of "surfactant" (Brito and Vaz, 1986). However, this increase in fluorescence is highly dependent on the subspecies composition of polysorbate, meaning higher degree of esterification induces a generally higher fluorescence signal, as demonstrated by Lippold et al. (2017). This phenomenon is supported by results of our current study. Placebos and non-shaken formulations of mAb1 showed constant apparent concentrations of PS20 as measured by FMA. Samples spiked with the non-hydrolyzed control reached the target concentration of 0.2 g•l^{-1}, while samples with lipase hydrolyzed PS20 showed reduced PS20 levels, from PPL F2 (approx. 90 % of target concentration) to PPL F6 (approx. 50 % of target concentration) to LPL (approx. 10 % of target concentration) treated PS20 in decreasing order (Fig. 6A), which were not in line with the expected 80 % PS20 level from the sample preparation (see 2.2.1 and 3.1). However, this corresponds well to the varying hydrolysis patterns observed for the three lipases (Fig. 2) and is in line with previous results (Glücklich et al., 2021). With decreasing higher-order species from PPL F2 to PPL F6 to LPL treated PS20 a decrease in the FMA signal is observed. This is in accordance with the results from Lippold et al. (2017) showing a higher sensitivity of the FMA to higher-order species of polysorbate (Lippold et al., 2017).

The mAb2 formulations required a higher target concentration of PS20 (0.4 g·l^{-1}) and showed similar trends. However, non-shaken mAb2 formulations spiked with PS20 showed a slight PS20 decrease over the study period of 120 h (Fig. 6B), while the corresponding placebos of

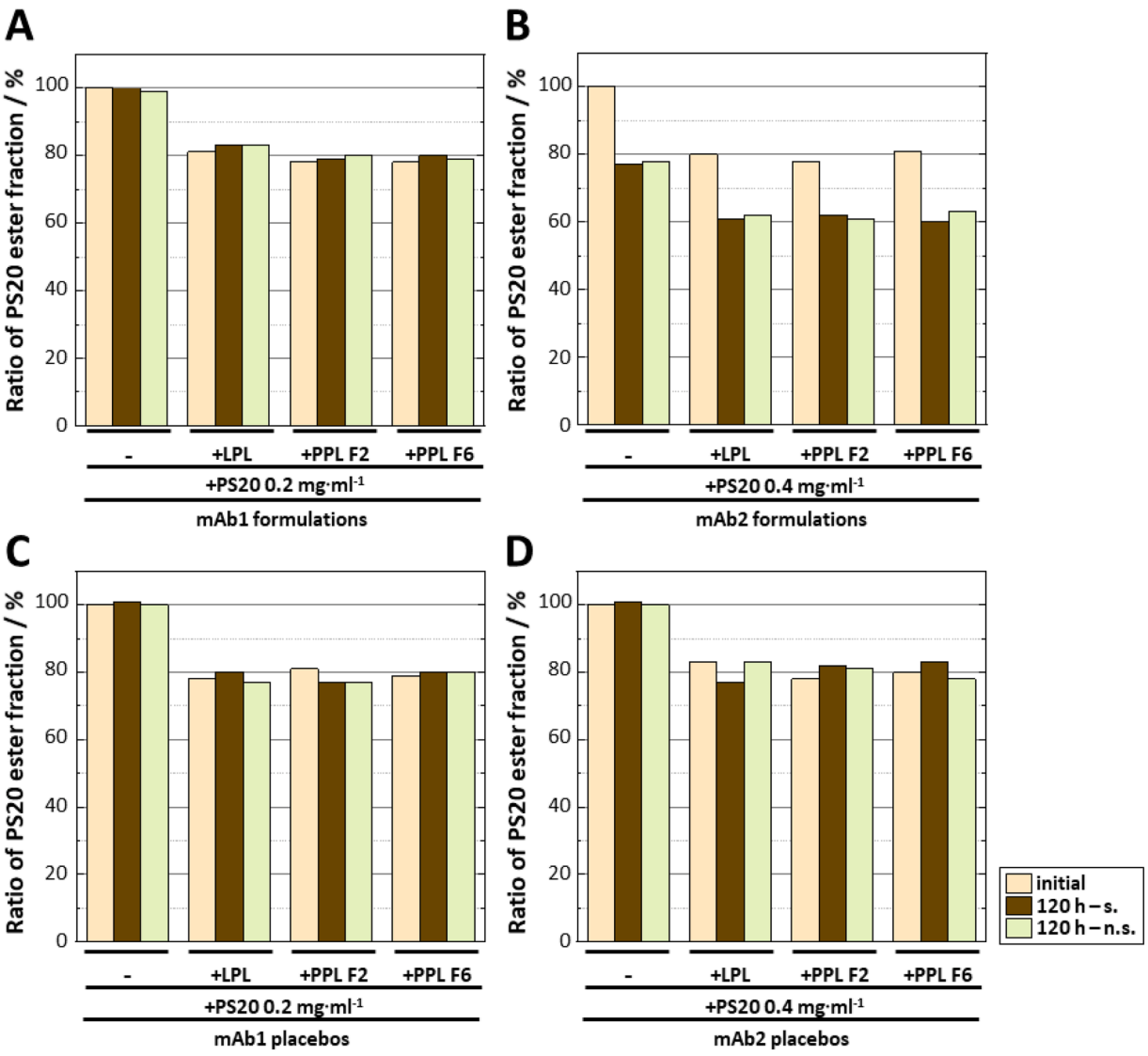

Fig. 7. Assessment of esterified polysorbate 20 (PS20) content via multi-peak charged aerosol detection reversed phase high-performance liquid chromatography (RP-HPLC—CAD). Esterified PS20 contents relative to the corresponding initial value [%] of the non-hydrolyzed PS20 controls are plotted for the tested formulations and placebos of mAb 1 (A and C, respectively) and mAb 2 (B and D, respectively). Formulations were either not spiked with polysorbate 20 (PS20; w/o PS20 data not shown), with PS20 non-hydrolyzed (-) or with enzymatically hydrolyzed PS20 (lipoprotein lipase (LPL), porcine pancreas lipase type II (PPL F2), porcine pancreas lipase type VI (PPL F6)). mAb1 formulations contained 20 $g{\cdot}l^{-1}$ protein and 0.2 $g{\cdot}l^{-1}$ PS20. While mAb2 formulations contained 25 $g{\cdot}l^{-1}$ protein and 0.4 $g{\cdot}l^{-1}$ PS20. Corresponding placebos did not contain any mAb, but the same amounts of PS. The different sampling time points and conditions (shaken = s.; non-shaken = n.s.) are shown in the legend at the bottom right.

mAb2 did not show this trend (Fig. 6D). Interestingly, for both mAb1 and mAb2 formulations shaking did induce an increase in FMA signal even in the samples without PS20 spike, leading to an apparent surfactant increase over the shaking period. This effect can be attributed to the possible interaction of the NPN dye with hydrophobic interfaces present in the sample (Kiese et al., 2008; Liu et al., 2013; Bhaumik and Hardwick; Martos et al., 2020). For example, the mAb2 sample formulated with 0.4 $g{\cdot}l^{-1}$ non-hydrolyzed PS20 showed after 120 h shaking the appearance of visible particles with strong opalescence (Fig. 3). The FMA, monitoring the PS20 content of this sample revealed a strong increase of the apparent PS20 amount, this is can be explained by the formation of hydrophobic protein particles that likely bind the dye and thus provide a false PS20 content. Therefore, this assay need to be improved. Due to these false positive PS concentrations caused by protein aggregates as well as the varying response of the FMA towards PS subspecies with different degree of esterification, we suggest using —RP-HPLC-CAD to determine the PS concentration of highly stressed samples like performed in this study where protein aggregation and particle formation is expected, and exact PS content determination is necessary.

Data from —RP-HPLC-CAD (Fig. 7) on the other hand demonstrated that the 20 % hydrolysis levels were well maintained over the course of the study for the mAb1 formulations and placebos as well as the mAb2 placebos spiked with lipase treated PS20. This analytical method uses a mixed mode column, which allows the removal of potentially interfering protein from the sample matrix and has an even response for the varying PS20 subspecies (Lippold et al. 2017). Interestingly, the mAb2 formulations showed that there was a loss of esters for all PS20 spiked samples whether they were shaken or not during their incubation at room temperature, which was also indicated by the FMA data of the non-shaken controls (Fig. 6B). This phenomenon can be explained by the lipolytic activity often found in biologics, which is induced by the presence of hard-to-remove host cell proteins, e.g. lipases and esterases (Chiu et al., 2017; Zhang et al., 2020; Hall et al., 2016). Since the presence and

activity of such HCPs is dependent on several factors, like the biologic itself, the purification process, and the buffer composition, it can be assumed that the mAb2 formulations had perceivable levels of such background hydrolytic activity (Chiu et al., 2017; Zhang et al., 2020; Hall et al., 2016). Residual activity of the used surrogate lipases after heat inactivation can be excluded since this effect was only observed for mAb2 formulations.

4. Summary and conclusion

There are multiple reports in the literature available demonstrating the varying enzymatic degradation specificity of PSs in liquid formulations of biologics (Chiu et al., 2017; Zhang et al., 2020; Park et al., 2017; Hall et al., 2016; Glücklich et al., 2021). However, so far, no comprehensive conclusions were drawn regarding the impact of such degradation for the stabilizing effect towards the API during interfacial stresses. Here we show that enzymatically-induced degradation of certain PS20 esters leads to variability in the protein stabilizing properties during shaking stress for two tested mAbs. Thereby, both mAbs showed similar trends regarding increased susceptibility towards shaking stress with varying severity.

To investigate the "remaining" protective effect of the degraded PSs, shaking was performed in vials with excessive headspace (3 ml headspace, 1 ml fill volume). Thereby shaking is an appropriate stress condition to apply mechanical and interfacial stress to the model mAbs and the headspace provides the necessary interfaces inducing protein particle formation, opalescence increases and visual changes in susceptible formulations (Kiese et al., 2008; Liu et al., 2013). In this study the two tested mAbs behaved differently to the applied stress. In the case of mAb1 the formation of HMWs measured by SEC were the strongest indication for increased shaking stress sensitivity upon specific PS degradation, while for mAb2 in addition to the HMW formation, visual effects, namely a strong formation of visual particles as well as opalescence were significantly more pronounced. This underlines that mAbs show distinctively different responses towards mechanical and interfacial stresses, which is expected due to their variability and structure and varying presence of aggregation prone regions (Li et al., 2011; Kant et al., 2017). However, this is out of scope of the current study. Furthermore, the described effects are reflected in the surfactant concentration needed to appropriately stabilize the mAb of interest as derived from the respective formulation development of both mAbs. For mAb1 a target PS20 concentrations of 0.2 $g{\cdot}l^{-1}$ is needed and for mAb2 0.4 $g{\cdot}l^{-1}$. Counterintuitively, the mAb formulation with the higher surfactant concentration performed overall worse than the one with the lower concentration also supporting the mAb structure-shaking stress susceptibility correlation, which need to be considered in future studies.

However, in general both mAbs showed similar overall trends regarding stabilizing properties for the varying spikes (without PS20, non-hydrolyzed PS20, PPL F2, PPL F6 and LPL). While the formulation in the absence of PS20 led to a fast protein particle formation and exceeding opalescence levels, best performance concerning formulation stability was achieved with the non-hydrolyzed PS20 spikes, which was expected, since these samples contained the highest amount of esterified PS20 subspecies. Controls with heat inactivated, non-hydrolyzed PS20 performed comparably indicating no relevant impact of the heat inactivation on the protective properties of PS20 for this study setup (data not shown). Both mAbs showed similar trends towards the differently lipase stressed PS20 spikes, regarding reduced shaking stability, in their respective formulations. PPL F6 hydrolysis induced the highest shaking stress susceptibility, followed by LPL and PPL F2, which had the lowest impact on formulation stability. One thing to note here, is that the overall amount of esterified and therefore surface active PS20 was kept constant for all stressed formulations (see Fig. 7). This translates to a more detrimental effect, if esters are degraded evenly followed by preferential degradation of multi-esters, while degradation of mainly mono-esters led to the weakest effect regarding instability for both mAb formulations.

It is difficult to compare these findings with reports from the literature, which describe actual enzymatic PS degradation mediated by HCPs, since varying mAbs with varying HCP profiles are investigated. This leads to distinct degradation patterns depending on the study. For example, Roy et al. (2021) presented a study, with evident hydrolytic HCP activity towards multi-esters, i.e. a preferential enzymatic degradation of multi-ester species of PS20, in a long-term (> 12 months) stability study spiked with different PS20 qualities and alternative surfactants. While the onset for particle formation varied depending on the surfactant, no comparison towards differently enzymatically hydrolyzed PS was possible. Other studies, like the one from Zhang et al. (2020), focused on the rapid PS degradation (within hours to days) in mAb formulations, that contained residual HCP with enzymatic effect towards PS, which showed preferential degradation of mono-esters in PS80 formulations. However, no data regarding the stability of the mAb were presented, especially long-term stability studies or, like in our study, at least accelerated shaking stress studies.

Tomlinson and colleagues (2020) chose a different approach to investigate the specific stabilizing properties of PS ester fractions (Tomlinson et al., 2020). Instead of using defined enzymatically hydrolyzed PS samples, the authors have purified and isolated selected subfractions of PS20 all-laurate and PS80 all-oleate and used them at varying concentrations for mAb formulations to test which fraction shows the highest stabilizing efficiency for agitation stress (Tomlinson et al., 2020). Interestingly, the isosorbide mono-laurate subfraction demonstrated the best stability performance (evaluated by visual inspection of the samples) (Tomlinson et al., 2020). Using a similar approach, namely the isolation of specific polysorbate fractions (Diederichs et al., 2023) concluded that fractions composed primarily by isosorbide-POE-monolaurates as well as the inherent polysorbate mixtures PS20 PLA and HP showed in the presented case study the best protein stabilization effects, whereas polysorbate fractions containing primarily higher-order esters showed less colloidal protection and increased particle formation. In both studies, isolated polysorbate fractions were used with "lower" amounts of free fatty acids in the surfactant fractions in comparison to normal PS20, as the fractions were additionally purified.

In this study, however, a model system was used simulating an enzymatic degradation profile and based on this model system the observed findings were different, because this case study shows that targeted degradation of mono-esters via PPL F2 had the highest protein stabilization effect of the three lipase-treated PS20 spikes in the presented case study, especially for mAb2. As an additional observation from the study of Tomlinson et al. (2020), the authors revealed that the fraction of sorbitan di-laurate performed better than sorbitan mono-laurate. A direct comparison of these studies is complex. For example, Tomlinson et al. (2020) used different matrix components compared to our study, which included various other fatty acid esters as found in compendial PS20, as well as the FFA released via the performed enzymatic degradation. The latter aspect, which is also relevant in the actual HCP mediated enzymatic PS degradation observed in drug product, might also contribute to the different impacts observed in the experimental setup of the current study, regarding the varying degradation fingerprints. Depending on the ester preferences of the used surrogate lipases, varying amounts of FFA are released, since hydrolysis of multi-esters releases more FFA than mono-esters. Recently, it was demonstrated that spiking of free fatty acids into mAb formulations can induce the formation of particles (Zhang et al., 2022). This supports our findings that formulations degraded with PPL F2 (mono-ester degradation) showed lower levels of HMWs (SEC measured) as well as lower opalescence during the shaking study compared to the LPL (preference for multi-ester degradation) and PPL F6 (esters evenly degraded) treated formulations. Additionally, data from other groups revealed that higher-order esters in polysorbates have reduced critical micelle concentration ranges and form on average "larger" micelles, which could be

beneficial for the solubility of FFA (Tomlinson et al., 2020; Nayem et al., 2019). This might explain the increased stability performance of PPL F2 treated samples, since they contained a higher ratio of di- and tri-esters. So, one can hypothesize from the two case studies, that the presence of polysorbate multi-ester fractions have a limited "protein stability" property, but a higher capacity to solubilize free fatty acids. These aspects could also contribute to a better performance of mAb1 in our study, as here a lower PS20 target concentration was used, which correspondingly leads to lower FFA levels in the lipase stressed formulations compared to mAb2. Nevertheless, an mAb dependent effect cannot be foreclosed, since in another study where the samples were exposed to long-term storage of 24 months at room temperature with hydrolytically active drug substance, only FFA particles were formed, depending on the PS degradation, without the presence of any mAb dependent particulates (Saggu et al., 2021).

In general, it has to be kept in mind that the data presented by Tomlinson et al. (2020), Diederichs et al. (2023) and Zhang et al. (2022) were generated in different setups compared to the current shaking study (Tomlinson et al., 2020; Zhang et al., 2022; Diederichs et al., 2023). While the former two groups used PS isolated fractions, which are not used in actual formulation development case study, the latter introduced additional FFA via spiking. In our approach we used surrogate lipases to introduce enzymatic degradation of compendial PS20, which should lead to degradation conditions, more comparable to actual formulations with realistic changes in PS20 ester distribution and FFA content. The proposed approach could be supportive for the predictivity of the experiment, since it also considers the interplay of the generated matrix, like a change of FFA solubility by variation of the remaining PS fractions.

Conclusively, the results of the current case study indicated that the reduction of the mono-esters is less detrimental for the two tested monoclonal antibodies. This information could be used for a first evaluation, if such PS degradation patterns driven by specific enzymatic degradation are observed during development. This is further underlined by the additional risk of FFA particle formation in formulations with multi-ester focused PS degradation, due to the overall increased amount of released FFA (Glücklich et al., 2020; Doshi et al., 2015). Both aspects give a hint that biopharmaceutical formulations with PS degradation focused on mono-esters are less likely to induce negative effects on the API (e.g. protein particle formation) or the drug product (e.g. visible FFA particles) quality, compared to degradation, which includes di- and tri-esters. This finding needs to be supported by additionally investigations. The observation that the presence of polysorbate multi-ester fractions have a limited protein stability property could be balanced by the fact that this polysorbate fraction could provide a higher solubilization property to fatty acids.

CRediT authorship contribution statement

Nils Glücklich: Investigation, Methodology, Formal analysis, Visualization, Writing – review & editing, Writing – original draft. **Stefan Carle:** Investigation, Methodology, Validation, Formal analysis, Visualization, Writing – review & editing, Writing – original draft. **Tim Diederichs:** Methodology, Validation, Formal analysis, Visualization, Writing – review & editing, Writing – original draft. **Julia Buske:** Conceptualization, Validation, Resources, Writing – review & editing. **Karsten Mäder:** Supervision, Project administration, Validation, Writing – review & editing. **Patrick Garidel:** Funding acquisition, Resources, Conceptualization, Project administration, Validation, Writing – review & editing.

Declaration of Competing Interest

The authors declare that they have no known competing financial interests or personal relationships that could have appeared to influence the work reported in this paper.

Data availability

Data will be made available on request.

Acknowledgments

We acknowledge Britta Schöder, Frank Hämmerling, Michael Hoang, Jean Schuchardt, Judith Cammerer, Simon Hötzel, Stefanie Glücklich, Judith Mittag, Timo Pydannah, Sina Rahnenführer, Torsten Schulz-Fademrecht and Mihaela Stumbaum for their technical support and data analysis, Martin Hessling, Holger Thie, and Kerstin Walke, Jan Visser for management supports.

References

Bee, J.S., Randolph, T.W., Carpenter, J.F., Bishop, S.M., Dimitrova, M.N., 2011. Effects of surfaces and leachables on the stability of biopharmaceuticals. J. Pharm. Sci. 100, 4158–4170.

Bhaumik, M.L. & Hardwick, R. Lattice work performed by excited molecules. J. Chem. 2023 S.

Brito, R.M.M., Vaz, W.L.C., 1986. Determination of the critical micelle concentration of surfactants using the fluorescent probe N-phenyl-1-naphthylamine. Anal. Biochem. 152, 250–255.

Chiu, J., et al., 2017. Knockout of a difficult-to-remove CHO host cell protein, lipoprotein lipase, for improved polysorbate stability in monoclonal antibody formulations. Biotechnol. Bioeng. 114, 1006–1015.

Diederichs, T., Mittag, J.J., Humphrey, J., Voss, S., Carle, S., Buske, J., Garidel, P., 2023. Existence of a superior polysorbate fraction in respect to protein stabilization and particle formation? Int. J. Pharm. 635, 122660.

Donbrow, M., Azaz, E., Pillersdorf, A., 1978. Autoxidation of polysorbates. J. Pharm. Sci. 67, 1676–1681.

Doshi, N., Demeule, B., Yadav, S., 2015. Understanding particle formation: solubility of free fatty acids as polysorbate 20 degradation byproducts in therapeutic monoclonal antibody formulations. Mol. Pharm. 12, 3792–3804.

Dwivedi, M., Blech, M., Presser, I., Garidel, P., 2018. Polysorbate degradation in biotherapeutic formulations: identification and discussion of current root causes. Int. J. Pharm. 552, 422–436.

EFSA (European Food Safety Authority), 2015. Panel on food additives and nutrient sources added to food (ANS) scientific opinion on the re-evaluation of polyoxyethylene sorbitan monolaurate (E 432), polyoxyethylene sorbitan monooleate (e 433), polyoxyethylene sorbitan monopalmitate (E 434), polyoxyethylene sorbitan monostearate (e 435) and polyoxyethylene sorbitan tristearate (E 436) as food additives. EFSA J. 13 (7), 4152, 74 pages.

Ehsan, M., Dehghan, N., Gholamreza, 2012. Effect of temperature on the critical micelle concentration and micellization thermodynamic of nonionic surfactants: polyoxyethylene sorbitan fatty acid esters. J. Chem. 9, 2268–2274 ny.

Evers, D.H., Schultz-Fademrecht, T., Garidel, P., Buske, J., 2020. Development and validation of a selective marker-based quantification of polysorbate 20 in biopharmaceutical formulations using UPLC QDa detection. J. Chromatogr. B 1157, 122287.

Garidel, P., Blech, M., Buske, J., Blume, A., 2021a. Surface tension and self-association properties of aqueous polysorbate 20 HP and 80 HP solutions: insights into protein stabilisation mechanisms. J. Pharm. Innov. 16, 726–734.

Garidel, P., Blech, M., Buske, J., Blume, A., 2021b. Surface tension and self-association properties of aqueous polysorbate 20 hp and 80 hp solutions: insights into protein stabilisation mechanisms. J. Pharm. Innov. 16, 726–734.

Glücklich, N., et al., 2020. An in-depth examination of fatty acid solubility limits in biotherapeutic protein formulations containing polysorbate 20 and polysorbate 80. Int. J. Pharm. 591, 119934.

Glücklich, N., Carle, S., Buske, J., Mäder, K., Garidel, P., 2021. Assessing the polysorbate degradation fingerprints and kinetics of lipases – how the activity of polysorbate degrading hydrolases is influenced by the assay and assay conditions. Eur. J. Pharm. Sci. 166, 105980.

Grabarek, A.D., et al., 2020. What makes polysorbate functional? impact of polysorbate 80 grade and quality on igg stability during mechanical stress. J. Pharm. Sci. 109, 871–880.

Hall, T., Sandefur, S.L., Frye, C.C., Tuley, T.L., Huang, L., 2016. Polysorbates 20 and 80 degradation by group XV lysosomal phospholipase A2 isomer X1 in monoclonal antibody formulations. J. Pharm. Sci. 105, 1633–1642.

Heider, M., Hause, G., Mäder, K., 2016. Does the commonly used pH-stat method with back titration really quantify the enzymatic digestibility of lipid drug delivery systems? A case study on solid lipid nanoparticles (SLN). Eur. J. Pharm. Biopharm. 109, 194–205.

Hewitt, D., et al., 2011. Mixed-mode and reversed-phase liquid chromatography–tandem mass spectrometry methodologies to study composition and base hydrolysis of polysorbate 20 and 80. J. Chromatogr. A 1218, 2138–2145.

Honemann, M.N., Wendler, J., Graf, T., Bathke, A., Bell, C.H, 2019. Monitoring polysorbate hydrolysis in biopharmaceuticals using a QC-ready free fatty acid quantification method. J. Chromatogr. B 1116, 1–8.

Kant, R.V.D., et al., 2017. Prediction and reduction of the aggregation of monoclonal antibodies. J. Mol. Biol. 429, 1244–1261.
Kiese, S., Papppenberger, A., Friess, W., Mahler, H.S., 2008. Not Stirred: mechanical stress testing of an IgG1 antibody. J. Pharm. Sci. 97, 4347–4366.
Kishore, R.S.K., et al., 2011. The degradation of polysorbates 20 and 80 and its potential impact on the stability of biotherapeutics. Pharm. Res. 28, 1194–1210.
Knoch, H., et al., 2021. Complex micellization behavior of the polysorbates tween 20 and tween 80. Mol. Pharm. 18, 3147–3157.
Labrenz, S.R., 2014. Ester hydrolysis of polysorbate 80 in mAb drug product: evidence in support of the hypothesized risk after the observation of visible particulate in mab formulations. J. Pharm. Sci. 103, 2268–2277.
Larson, N.R., et al., 2020. Comparison of polysorbate 80 hydrolysis and oxidation on the aggregation of a monoclonal antibody. J. Pharm. Sci. 109, 633–639.
Li, Y., Mach, H., Blue, J.T., 2011. High throughput formulation screening for global aggregation behaviors of three monoclonal antibodies. J. Pharm. Sci. 100, 2120–2135.
Lippold, S., et al., 2017. Impact of mono- and poly-ester fractions on polysorbate quantitation using mixed-mode HPLC-CAD/ELSD and the fluorescence micelle assay. J. Pharm. Biomed. 132, 24–34.
Liu, L., Qi, W., Schwartz, D.K., Randolph, T.W., Carpenter, J.F., 2013. The effects of excipients on protein aggregation during agitation: an interfacial shear rheology study. J. Pharm. Sci. 102, 2460–2470.
Martos, A., et al., 2017. Trends on analytical characterization of polysorbates and their degradation products in biopharmaceutical formulations. J. Pharm. Sci. 106, 1722–1735.
Martos, A., et al., 2020. Novel high-throughput assay for polysorbate quantification in biopharmaceutical products by using the fluorescent dye dil. J. Pharm. Sci. 109, 646–655.
Nayem, J., et al., 2019. Micellar morphology of polysorbate 20 and 80 and their ester fractions in solution via small-angle neutron scattering. J. Pharm. Sci. 109, 1498–1508.
Park, J.H., et al., 2017. Proteomic analysis of host cell protein dynamics in the culture supernatants of antibody-producing CHO cells. Sci. Rep. 7, 44246 uk.
Ph.Eur, 2020. European Pharmacopoeia. Council of Europe.
Rayaprolu, B.M., Strawser, J.J., Anyarambhatla, G., 2018. Excipients in parenteral formulations: selection considerations and effective utilization with small molecules and biologics. Drug Dev. Ind. Pharm. 44, 1–22.
Roy, I., et al., 2021. Polysorbate degradation and particle formation in a high concentration mab: formulation strategies to minimize effect of enzymatic polysorbate degradation. J. Pharm. Sci. https://doi.org/10.1016/j.xphs.2021.05.012.
Saggu, M., et al., 2021. Extended characterization and impact of visible fatty acid particles - a case study with a mAb product. J. Pharm. Sci. 110, 1093–1102.
Sluzky, V., Klibanov, A.M., Langer, R., 1992. Mechanism of insulin aggregation and stabilization in agitated aqueous solutions. Biotechnol. Bioeng. 40, 895–903.
Tomlinson, A., Zarraga, I.E., Demeule, B., 2020. Characterization of polysorbate ester fractions and implications in protein drug product stability. Mol. Pharm. 17, 2345–2353.
USP-NF, 2020. The United States Pharmacopeia. The National Formulary. United States Pharmacopeial Convention, Inc.
Vanderlaan, M., et al., 2018. Experience with host cell protein impurities in biopharmaceuticals. Biotechnol. Progr. 34, 828–837.
Wang, W., 1999. Instability, stabilization, and formulation of liquid protein pharmaceuticals. Int. J. Pharm. 185, 129–188.
Weber, J., Buske, J., Mäder, K., Garidel, P., Diederichs, T., 2023. Oxidation of Polysorbates – An Underestimated Degradation Pathway? Int J Pharm X 6, 100201. https://doi.org/10.1016/j.ijpx.2023.100202.
Wuchner, K. et al. Industry perspective on the use and characterization of polysorbates for biopharmaceutical products part 1: survey report on current state and common practices for handling and control of polysorbates. J. Pharm. Sci. 2023 111, 1280–1291.
Zhang, S., Xiao, H., Molden, R., Qiu, H., Li, N., 2020. Rapid polysorbate 80 degradation by liver carboxylesterase in a monoclonal antibody formulated drug substance at early stage development. J. Pharm. Sci. 109, 3300–3307.
Zhang, S., et al., 2022a. Identification of the specific causes of polysorbate 20 degradation in monoclonal antibody formulations containing multiple lipases. Pharm. Res. 39, 75–87.
Zhang, J., He, J., Smith, K.J., 2022b. Fatty acids can induce the formation of proteinaceous particles in monoclonal antibody formulations. J. Pharm. Sci. 111, 655–662.